Carbohydrate Polymers 117 (2015) 230–235

Contents lists available at ScienceDirect

Carbohydrate Polymers

journal homepage: www.elsevier.com/locate/carbpol

Flexible conductive polypyrrole nanocomposite membranes based on bacterial cellulose with amphiphobicity

Lian Tang[1], Jinlu Han[1], Zhenlin Jiang, Shiyan Chen**, Huaping Wang*

State Key Laboratory for Modification of Chemical Fibers and Polymer Materials, Key Laboratory of High Performance fibers and products (Ministry of Education), College of Materials Science and Engineering, Donghua University, Shanghai, 201620, PR China

ARTICLE INFO

Article history:
Received 15 August 2014
Received in revised form
16 September 2014
Accepted 18 September 2014
Available online 28 September 2014

Keywords:
Bacterial cellulose
Polypyrrole
Nanocomposite
Amphiphobicity

ABSTRACT

Flexible conductive polypyrrole nanocomposite membranes based on bacterial cellulose (BC) with amphiphobicity have been successfully prepared through in situ chemical synthesis and then infiltrated with polysiloxane solution. The results suggested that polypyrrole (PPy) nanoparticles deposited on the surface of BC formed a continuous core–shell structure by taking along the BC template. After modification with polysiloxane, the surface characteristics of the conductive BC membranes changed from highly hydrophilic to hydrophobic. The AFM images revealed that the roughness of samples after polysiloxane treatment increased along with the increase of pyrrole concentration. The contact angles (CAs) data revealed that the highest water contact angle and highest oil contact angle are 160.3° and 136.7°, respectively. The conductivity of the amphiphobic membranes with excellent flexibility reached 0.32 S/cm and demonstrated a good electromagnetic shielding effectiveness with an SE of 15 dB which could be applied in electromagnetic shielding materials with self-cleaning properties. It opened a new field of potential applications of BC materials.

1. Introduction

The requirement for new technologies that demand materials with excellent overall performance has driven materials research towards the development of novel multi-functional nanoscaled composite materials. For this reason, the improvement in mechanical properties of conducting polymers and multi-functionalization of materials are still focus for innovation and research (Nystrom et al., 2010).

During the past three decades, a wide variety of electrically conducting polymers have been extensively studied due to their exclusive physical properties. Polypyrrole (PPy) is one of most potential conducting polymer for its high electrical conductivity, easy synthesis and non-poisonous property (Omastova & Micusik, 2012). It was reported that PPy could be a kind of valuable material with potential application as gas sensors (Lange, Roznyatovskaya, & Mirsky, 2008; Shukla, 2013), pH sensors (Pankaj, Kumar, & Sukhjeet, 2012), mechanical sensors (Tjahyono, Aw, & Travas-Sejdic, 2012), biomedical field (Hardy, Lee, & Schmidt, 2013; Wang et al., 2014), electromagnetic shielding (Kaur, Ishpal, & Dhawan, 2012), electronics (Pickup et al., 1997), electrochromic devices (Takagi, Makuta, Veamatahau, Otsuka, & Tachibana, 2012), fuel cells (Yuan, Ding, Wang, & Ma, 2013), antistatic materials (Varesano & Tonin, 2008). However, the application of PPy is restricted by its poor mechanical properties. In order to solve this problem, considerable work on preparation of various PPy composite materials has been done in recent years. It has been reported that a variety of polymeric materials with excellent physical properties are available as good matrixes for PPy, such as cellulose (Wang et al., 2013), polyamide (Granato, Bianco, Bertarelli, & Zerbi, 2009), polyester (Yildiz, Usta, & Gungor, 2012), polyoxyphenylene (Aguilar-Hernandez, Skarda, & Potje-Kamloth, 1998), plastic (Kawakita, Hashimoto, & Chikyow, 2013) and rubber (Tjahyono, Aw, & Travas-Sejdic, 2012). However, the current raw material shortcomings prompt us to find sustainable and recyclable materials with performance at the same level or better than conventional materials which are non-renewable. As one of the most abundant renewable eco-friendly resources, cellulose has drawn more and more attention (Grombe, 2009). Bacterial cellulose (BC) is a kind of cellulose obtained from bacteria which exhibits a three-dimensionally porous network and diameters of nanofibrils are 10–100 nm (Marins, Soares, Barud, & Ribeiro, 2013). Compared to natural cellulose, BC presents the attractive features including high crystallinity, high degree of polymerization, high purity, high

* Corresponding author. Tel.: +86 21 67792950; fax: +86 21 67792958..
** Corresponding author.
E-mail address: wanghp@dhu.edu.cn (H. Wang).
[1] These authors equally contributed to this work.

http://dx.doi.org/10.1016/j.carbpol.2014.09.049
0144-8617/

tensile strength, high biocompatibility and moldability during the formation process (Klemm, Schumann, Udhardt, & Marsch, 2001; Sen, Hamelin, Bru-Adan, Godon, & Chandra, 2008). BC has been an excellent template to synthesize nano-materials with abundant active hydroxyl, hyperfine structure through its three-dimensional and porous structure, thus obtained various new functional materials (Ashori, Sheykhnazari, Tabarsa, Shakeri, & Golalipour, 2012; Gutierrez, Tercjak, Algar, Retegi, & Mondragon, 2012; Hu, Chen, Yang, Li, & Wang, 2014; Lin, Guan, & Huang, 2013; Martins et al., 2013; Wen et al., 2013; Zheng et al., 2014).

It is far from approving to give the PPy composites with good mechanical property and good electrical performance. Moreover, the electrical performance of PPy is unstable in some atmospheric conditions which may be a weakness when applied. The hydrophilic nature of the BC membrane and its nanocomposites not only causes dimensional instability but also limits the usage time of the materials. On the other hand, materials with amphiphobicity will possess self-clean property which is very useful for outdoor goods. Thus, it is of great importance to fabricate the conductive nanocomposites with high amphiphobicity. The factors that influence the amphiphobicity of the materials are the degree of roughness and the material's surface energy. On the one hand, the water and oil repellency are improved by increasing the degree of roughness. The formation of the micro/nanostructures structure is conducive to refrain from being bedewed (Feng et al., 2003; Jung & Bhushan, 2006; Lafuma & Quere, 2003). Materials without any chemical modification for low surface energy can show excellent hydrophobic through reasonable surface design of the construction (Zhu & Jin, 2005). On the other hand, the surface characteristics of the materials can be changed by surface treatment agents with low surface energy such as fluorine-based or silicone-based silanes (O'Lenick, 2000). Compared to fluoride, although it has higher surface energy, polysiloxane is still attractive because of its low cost and simple technology (Pan et al., 2012).

In this paper, conductive BC membrane via in situ chemical synthesis of PPy nanoparticles on the surface of BC nanofibrils with amphiphobic surface properties were prepared. The effect of the pyrrole concentration was taken into consideration to find the optimal reaction conditions. In addition, the surface wettability, the conductivity, thermostability, electromagnetic shielding effectiveness of composite membranes were investigated.

2. Experimental

2.1. Materials and instruments

The preparation and characterization of bacterial cellulose (BC) membranes (4 cm × 5 cm) have been expatiated in our previously published report (Yan, Chen, Wang, Wang, & Jiang, 2008). The membranes were washed thoroughly with distilled water until pH 7. Pyrrole (Py) and iron (III) chloride hexahydrate ($FeCl_3{\cdot}6H_2O$) were purchased from Sinopharm Chemical Reagent Co. Ltd. Methyltrimethoxysilane (MTMS) and hydroxy-terminated polydimethylsiloxane (M_n = 2000) (PDMS-OH) were purchased from Quzhou Ruilijie Chemical Co. Ltd. All reagents were of analytical grade and were used without any further purification.

The electrical conductivity of membranes was measured at room temperature by the standard four-probe method. The morphologies of membranes were observed using a S-4800 field emission scanning electron microscope (FE-SEM) after coating with conductive gold. The Fourier transform-infrared (FT-IR) spectra were recorded on a NEXUS-670 FTIR spectrometer using the pressing potassium bromide troche method. The water contact angle (WCA) and oil contact angle (OCA) of the resultant samples were measured with an OCA40 contact angle meter. Atomic force microscopy (AFM) images were taken on the NanoScope IV AFM. The shielding effectiveness of samples was investigated on DR-S02 shielding effectiveness tester. The thermogravimetric analysis (TGA) was recorded on a TG 209 F1 lris thermogravimetric analyzer.

2.2. Preparation of PPy/BC nanocomposite membrane

After mechanical pressing to remove the physically adsorbed water, three pieces of water-wet BC membranes (containing about 50 mg dry BC each piece) were immersed in the pyrrole solution with concentrations varying from 0.01 to 0.09 mol/L under magnetic stirring. After the solution were stirred for 2 h, an aqueous solution of iron (III) chloride hexahydrate ($FeCl_3{\cdot}6H_2O$) was added dropwise to initiate polymerization. The molar ratio of Py:$FeCl_3{\cdot}6H_2O$ was 1:2.3. The mixture was stirred at room temperature for another 120 min. After the reaction completed, the obtained products were rinsed thoroughly with alcohol and distilled water in turn to remove excess reagents and other byproducts. Finally, the membranes were freeze-dried for 24 h. The composites obtained through different monomer concentrations of 0.01 mol/L, 0.03 mol/L, 0.05 mol/L, 0.07 mol/L and 0.09 mol/L were coded as PPy/BC1, PPy/BC2, PPy/BC3, PPy/BC4 and PPy/BC5, respectively. Purified BC membrane without further treatments was coded as pure BC.

2.3. Preparation of polysiloxane sols

The preparation process of polysiloxane sols is shown in Scheme S1. MTMS was hydrolyzed under catalysis of HCl and generated silanol groups. The hydrolyzed MTMS reacted with PDMS-OH to form a cross-linked structure. The silanol groups obtained from hydrolysis of MTMS could react with any one of silanol groups, and might not participate in the reaction as well. In this reaction, MTMS acted as a crosslinking center, and the flexibility of coating was afforded by PDMS-OH. Thus, the flexibility and curing performance of coating was effected by the mass ratio of MTMS:PDMS-OH. In this reaction, an optimized MTMS:PDMS-OH:H_2O:HCl (0.1 mol/L) mass ratio of 66.7:17.5:18:2 was used. The sols were placed in a round-bottomed flask with a magnetic stirrer for about 6 h at 60 °C (Bewilogua, Bialuch, Ruske, & Weigel, 2011). The prepolymeric polysiloxane solution was prepared by dispersing polysiloxane in isopropanol with a concentration of 50 wt% under stirring strongly for 10 min at room temperature.

3. Results and discussion

3.1. Preparation of flexible conductive nanocomposite membranes with amphophobicity

Fig. 1 shows the schematic preparation process of conductive nanocomposite membranes with amphiphobicity. When the flexible nano-porous BC membranes are immersed in the aqueous pyrrole solution, the pyrrole monomers can permeate the network of the BC membrane. Meanwhile, the high number of hydroxyl groups of BC can make the monomers uniformly distributed on the surface of BC nanofibers by forming hydrogen bonds with pyrrole (Wang et al., 2013). After addition of BC membranes impregnated with pyrrole into the aqueous $FeCl_3$ solution, the PPy formed on the surface of BC nanofibers by in situ polymerization (Scheme S2). The prepared PPy/BC samples were immersed into prepolymeric polysiloxane solution for 30 min under magnetic stirring at 40 °C. The samples were then dried in air-blown drier at 120 °C for 12 h. Thus, the polysiloxane macromolecule anchored on nanofibers uniformly by the surplus silanol groups of polysiloxane, forming a cross-linked siloxane network. The polysiloxane coated samples of pure BC, PPy/BC1, PPy/BC2, PPy/BC3, PPy/BC4 and PPy/BC5 were

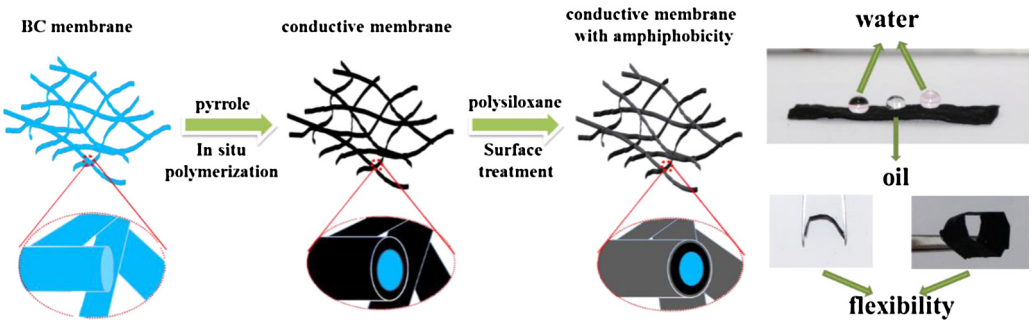

Fig. 1. Preparation process of conductive nanocomposite membrane with amphiphobicity.

referred to as SBC, SPPy/BC1, SPPy/BC2, SPPy/BC3, SPPy/BC4 and SPPy/BC5, respectively.

3.2. Morphology and surface wettability

Morphology and surface wettability of the membranes were investigated using FE-SEM and contact angle meter. Fig. 2 shows the FE-SEM images of pure BC, PPy/BC4 and SPPy/BC4. From the images, we can see that the exquisite three-dimensional network structure maintained through the composite process and surface treatment. The obvious change is the diameters of fibers varied from about 50 nm to 100 nm, and then to 150 nm. It can be explained that the fiber surface was firstly coated with continuous PPy, thus leading to the increase of the fiber diameter. The diameters of the coated BC fibers with PPy were further increased by the polysiloxane coating. The inset of Fig. 2c shows the energy-dispersive spectrum (EDS) of SPPy/BC4. There are N and Si elements in the composite, which indicated that PPy have been fabricated successfully by in situ synthesis and the fibers are coated with polysiloxane.

Fig. 3 shows the FE-SEM images of pure BC, SBC, SPPy/BC1, SPPy/BC2, SPPy/BC3, SPPy/BC4 and SPPy/BC5 (the FE-SEM images of PPy/BC nanocomposites through different pyrrole concentrations are shown in Figure S1 in the Supplementary data). When the pyrrole concentration is 0.01 mol/L, some PPy particles discontinuously disperse on the BC nanofibers (Fig. 3b, Figure S1b). With the increase of pyrrole concentration from 0.01 to 0.09 mol/L, it is found that the PPy nanoparticles deposited on the surface of fibers are connected to make up a continuous core–sheath structure by taking along BC templates (Hu, Chen, Yang, Liu, & Wang, 2011). The hydrogen bands between BC and pyrrole rings might play the guiding role of fabricating the continuous core–sheath structure and avoid to form the large-scale aggregate. When the pyrrole concentration was increased to 0.07 mol/L, the least PPy aggregates can be observed (Fig. 3e, Figure S1e). While further increased the pyrrole concentration to 0.09 mol/L, more PPy aggregates formed on the surface of BC membranes (Fig. 3f, Figure S1f). The insets of Fig. 3 show the photographs of water (up) and oil (down) drops on samples. When placed water or glycol droplets on BC surface, droplets

Table 1
WCAs, OCAs and RMS roughness of the amphiphobic SBC and SPPy/BC composites.

Samples	WACs (deg)	OACs (deg)	RMS roughness (nm)
SBC	100.6	79.2	41.1
SPPy/BC1	136.7	88.2	60.3
SPPy/BC2	142.5	124.5	122.5
SPPy/BC3	147.6	128.1	176.3
SPPy/BC4	151.0	135.5	401.8
SPPy/BC5	160.3	136.7	469.2

were immediately absorbed which indicated good amphiphilicity for BC. After surface treatment by polysiloxane, the average WCA for BC increased to 100.6° and the average OCA for SBC is about 79.2° (Table 1). The phenomena demonstrated that amphiphilicity was obviously decreased. When the BC surface was coated with PPy, and subsequently treated with polysiloxane, the average WCA and OCA further increased from 136.7° to 160.3° and 88.2° to 136.7° with the increase of pyrrole concentration (Table 1), respectively. The SPPy/BC composite membranes completely achieved change from amphiphilicity to amphiphobicity. On the one hand, polysiloxane is well known as an excellent amphiphobic material. It can provide surface wettability of the membranes changing them from amphiphilic to amphiphobic. On the other hand, the hierarchical micro/nanostructure of PPy formed on the three-dimentional network structure of BC substrate which sustained the spheres like a shelf (Zhang et al., 2011). The structure can result in reduction of the contact area of droplets and fibers (Tang, Wang, & He, 2009) as well as a decline in permeability of droplets which can be confirmed by the following discussion of surface roughness.

3.3. Surface roughness of membranes

Surface roughness has important influence on the CAs of the composite membranes. The AFM images of SBC, SPPy/BC1, SPPy/BC2, SPPy/BC3, SPPy/BC4 and SPPy/BC5 are shown in Fig. S2. The calculated Root-Mean-Square (RMS) roughness of SBC is 41.1 nm (Table 1), which is higher than that of glass plate sample (around 2 nm) (Janik, Kucharski, Sobolewska, & Barille, 2010; Wang

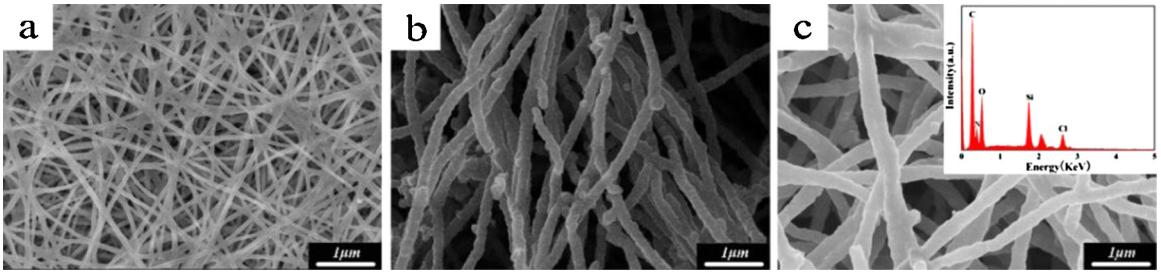

Fig. 2. FE-SEM images of (a) pure BC, (b) PPy/BC4 and (c) SPPy/BC4, the inset shows the EDS image of SPPy/BC4.

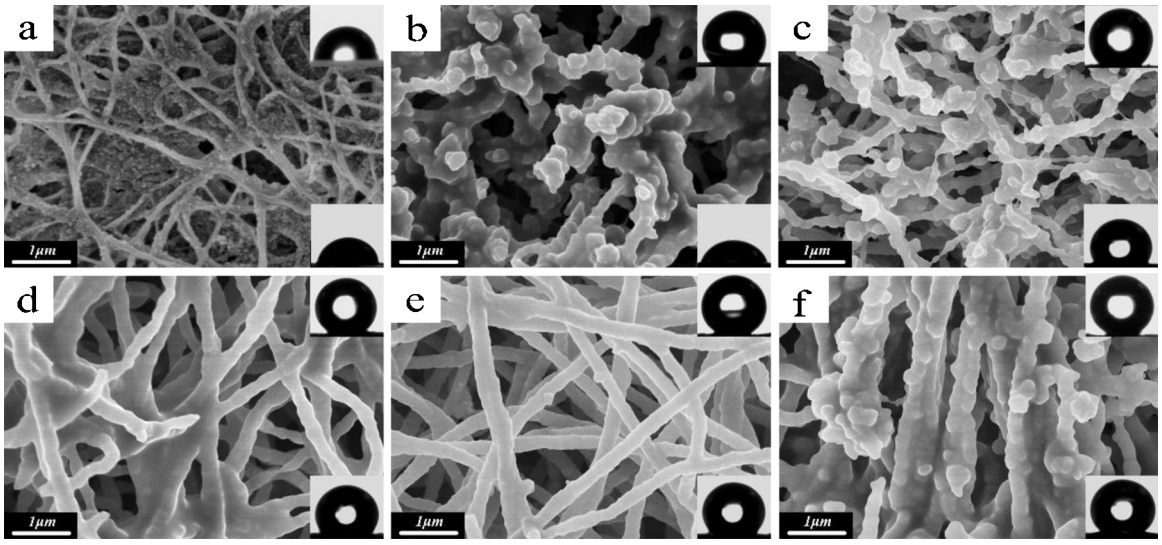

Fig. 3. FE-SEM images of (a) SBC, (b) SPPy/BC1, (c) SPPy/BC2, (d) SPPy/BC3, (e) SPPy/BC4 and (f) SPPy/BC5, respectively. The insets show the photographs of water (up) and oil (down) drops on samples.

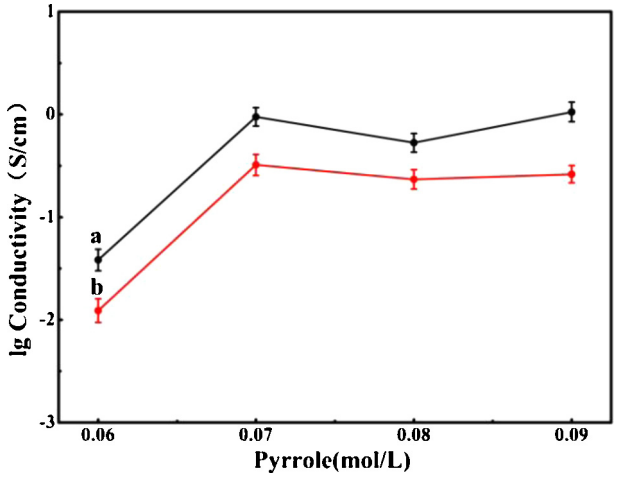

Fig. 4. Electrical conductivity of PPy/BC (a) and SPPy/BC (b) composite membranes prepared by different pyrrole concentrations at room temperature.

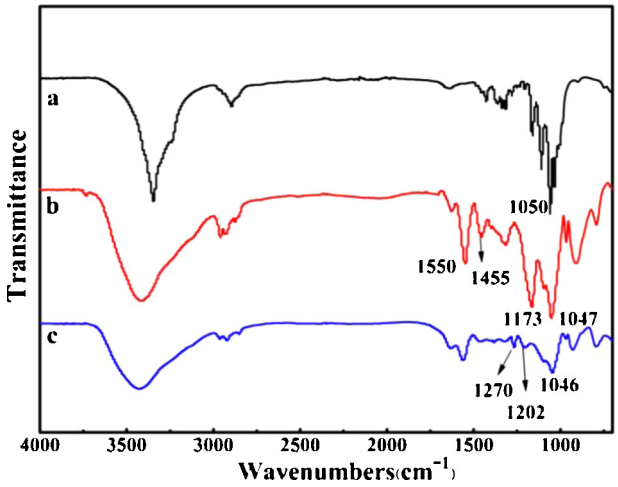

Fig. 5. FTIR spectra of pure BC (a), PPy/BC4 (b) and SPPy/BC4 (c).

& He, 2006). The difference is due to the three-dimentional network structure of BC (Zhang et al., 2011). The formation of the hierarchical nanostructure results in a thick air layer, which keeps the water droplet from contact with the fibers substrate (Tang et al., 2009). After the coating with PPy and polysiloxane, the top surface layers of the five samples were rougher than SBC and the RMS roughness data of the membranes are shown in Table 1. From the data, we can see that the RMS roughness of membranes increases along with the increase of the pyrrole concentration which indicates bigger value of CAs (Zhu & Jin, 2005). The results are consistent with the CAs discussed in section of surface wettability.

3.4. Electrical conductivity

Fig. 4 shows the electrical conductivity of PPy/BC and SPPy/BC composite membranes with different pyrrole concentrations from 0.06 to 0.09 mol/L. It is revealed that the electrical conductivity firstly increases with the increase of monomer concentration and then reached a plateau. When the pyrrole concentration was 0.07 mol/L, the conductivity of PPy/BC4 and SPPy/BC4 were 0.94 S/cm and 0.32 S/cm, respectively. The results demonstrate that an unbroken core–sheath structure to form an intact conductive pathway is essential in obtaining optimum electrical conductivity. After surface treatment by polysiloxane, a slight decrease of electrical conductivity is observed. It is because the interaction of polysiloxane and PPy may led to the fracture of the PPy conjugated chain and at the same time, the doping system may be undermined to some extent (Bozkurt, Parlak, Ercelebi, & Toppare, 2002). However, polysiloxane only covers the fibers on the surface layer and the damaging effect is only superficial. Thus the conductivity of membranes before and after treatment is in the same order of magnitude.

3.5. FTIR spectroscopy

The structures of the prepared composites are further confirmed by FTIR spectroscopy (Fig. 5). As shown in Fig. 5a, the characteristic IR peaks of pure BC shows three major bands: two bands located at around 3350 cm^{-1} and 2900 cm^{-1} are attributed to hydroxyl and C—H of carbohydrate stretching vibration. A sharp band at 1050 cm^{-1} is attributed to hydroxyl and C—O—C of carbohydrate stretching vibration. The curve of PPy/BC4 (Fig. 5b) exhibits the

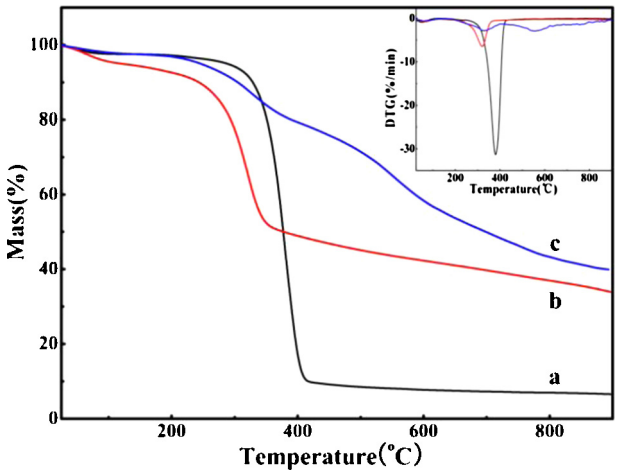

Fig. 6. TGA curves of (a) pure BC, (b) PPy/BC4 and (c) SPPy/BC4, the inset shows DTG curves of (a) pure BC, (b) PPy/BC4 and (c) SPPy/BC4.

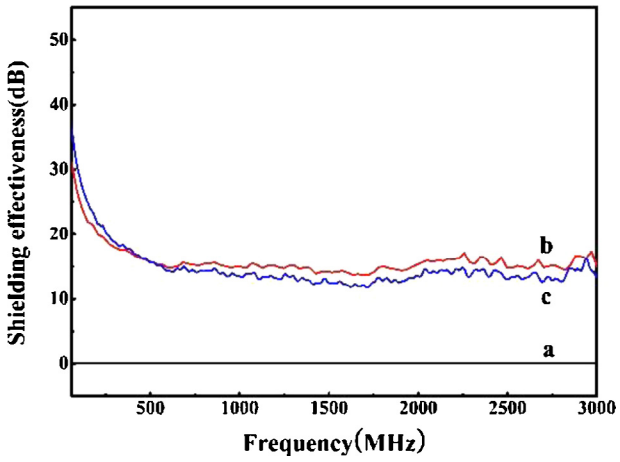

Fig. 7. Shielding effectiveness curves of (a) pure BC, (b) PPy/BC4 and (c) SPPy/BC4.

characteristic peaks belong to polypyrrole at around 1550 cm^{-1} and 1455 cm^{-1} corresponding to C—N stretching vibration and C—C stretching vibrations in the pyrrole ring (Chen et al., 2013; Müller, Rambo, Recouvreux, Porto, & Barra, 2011). Except for these peaks, a new absorption peak located at 1270 cm^{-1} can be observed in SPPy/BC4 (Fig. 5c), corresponding to the stretching vibration of Si—CH_3 bonds. However, the peak at 1173 cm^{-1} corresponding to the characteristic peak of PPy weakens and moves to higher wave numbers (1202 cm^{-1}), which indicates that PPy is covered by polysiloxane. Because the peak of C—O—C bands and the peak of Si—O—Si bands may superpose each other, the peak around at 1046 cm^{-1} changes from sharp to dull (Pan et al., 2012; Salazar-Hernández, Alquiza, Salgado, & Cervantes, 2010).

3.6. Thermogravimetric analysis

Fig. 6 depicts the thermograms of BC and its components. The weight loss before 100 °C is due to the moisture evaporation. It is observed that the pure BC (Fig. 6a) lost its weight quickly starting from 350 °C up to 400 °C and the velocity of mass loss accelerated as the temperature reached 380 °C. Fig. 6b shows the TGA curve of PPy/BC4. We can see that the onset thermal degradation temperature starts at around 300 °C (Fig. 6b) and the highest rate of weight loss occurs at 320 °C. Compared with the pure BC, the thermal stability of PPy/BC4 decreased. It is mainly because the interaction coming from hydroxyl groups was weakened and the crystal structure of BC was partly destroyed during the process of in-situ synthesis. The weight loss of PPy/BC4 is less than pure BC, it might attribute to residuary PPy. Two major weight losses are found in the TGA curve of SPPy/BC4 (Fig. 6c and inset), the one from 270 to 360 °C is mainly due to the thermolysis of BC. The one from 520 to 590 °C is ascribed to the decomposition of Si—C bonds. Compared with the PPy/BC4, the weight loss of SPPy/BC4 is less which may come from the skin-core structure coated by polysiloxane with excellent heat-resistant in SPPy/BC composites.

3.7. Electromagnetic shielding analysis

When electromagnetic wave encounter a material interface, some of the wave is reflected and some is transmitted. The electromagnetic wave entering the material might be absorbed if the material properties allow, or it can pass through virtually undiminished (Håkansson, Amiet, Nahavandi, & Kaynak, 2007). Generally, almost all the radiation can penetrate an insulating material not reflected from the surface, and almost all radiation can be reflected or absorbed by a conductive material (Wang & Jing, 2005). Materials such as metals usually stop the radiation from penetrating though reflecting, and material such as conductive polymer would absorb the radiation when the radiation penetrated it. The frequency dependence of microwave absorption is a main criterion in selecting materials for electro-magnetic interference (EMI) shielding applications. Fig. 7 reveals that pure BC (Fig. 7a) could not impede transmission of the radiation. The absorption dominated shielding effectiveness of PPy/BC4 (Fig. 7b) and SPPy/BC4 (Fig. 7c) is around 15 dB. The results indicate that PPy/BC nanocomposite membrane and its amphiphobic one can be used as an effective, lightweight and flexible EMI shielding material (Li et al., 2006). However, the shielding effectiveness of SPPy/BC4 display a somewhat lower than PPy4/BC, this is attributed to decrease in conductivity, in agreement with the EMI shielding theory (Azadmanjiri, Hojati-Talemi, Simon, Suzuki, & Selomulya, 2011).

4. Conclusion

We have successfully prepared flexible conductive nanohybrid membrane with amphiphobic surface based on BC by in situ oxidative polymerization of PPy and subsequent polysiloxane modification. The ultrafine network structure and hydroxyl groups of BC nanofibers constitute an effective nanoreactor for the reaction. It was found that the PPy particles uniformly deposited on the surface of BC nanofiber connected to form a continuous core–shell structure by taking along the BC template under the optimized condition. The obtained SPPy/BC4 membrane showed the highest amphiphobicity with a WCA of 160.3° and an OCA of 136.7° and demonstrated a good electromagnetic shielding effectiveness with an SE of 15 dB. This work would provide a straightforward method to prepare flexible films with high conductivity and high amphiphobicity which could be applied in electromagnetic shielding materials with self-cleaning properties. It also opens a new thought of potential applications of BC materials.

Acknowledgments

This work was financially supported by the Fundamental Research Funds for the Central Universities, the National Natural Science Foundation of China (51273043), Project of the Action on Scientists and Engineers to Serve Enterprises (2009GJE20016), and the Fundamental Research Funds for the Central Universities (2232013D3-01).

Appendix A. Supplementary data

Supplementary material related to this article can be found, in the online version, at http://dx.doi.org/10.1016/j.carbpol.2014.09.049.

References

Aguilar-Hernandez, J., Skarda, J., & Potje-Kamloth, K. (1998). Insulator–semiconductor composite polyoxyphenylene–polypyrrole: Electrochemical synthesis, characterization and chemical sensing properties. *Synthetic Metals*, *95*(3), 197–209.

Ashori, A., Sheykhnazari, S., Tabarsa, T., Shakeri, A., & Golalipour, M. (2012). Bacterial cellulose/silica nanocomposites: Preparation and characterization. *Carbohydrate Polymers*, *90*(1), 413–418.

Azadmanjiri, J., Hojati-Talemi, P., Simon, G. P., Suzuki, K., & Selomulya, C. (2011). Synthesis and electromagnetic interference shielding properties of iron oxide/polypyrrole nanocomposites. *Polymer Engineering & Science*, *51*(2), 247–253.

Bewilogua, K., Bialuch, I., Ruske, H., & Weigel, K. (2011). Preparation of a-C:H/a-C:H:Si:O and a-C:H/a-C:H:Si multilayer coatings by PACVD. *Surface & Coatings Technology*, *206*(4), 623–629.

Bozkurt, A., Parlak, M., Ercelebi, C., & Toppare, L. (2002). Conduction mechanism in H-type polysiloxane–polypyrrole block copolymers. *Journal of Applied Polymer Science*, *85*(1), 52–56.

Chen, S., Zhou, B., Hu, W., Zhang, W., Yin, N., & Wang, H. (2013). Polyol mediated synthesis of ZnO nanoparticles templated by bacterial cellulose. *Carbohydrate Polymers*, *92*(2), 1953–1959.

Feng, L., Song, Y. L., Zhai, J., Liu, B. Q., Xu, J., Jiang, L., et al. (2003). Creation of a superhydrophobic surface from an amphiphilic polymer. *Angewandte Chemie International Edition*, *42*(7), 800–802.

Granato, F., Bianco, A., Bertarelli, C., & Zerbi, G. (2009). Composite polyamide 6/polypyrrole conductive nanofibers. *Macromolecular Rapid Communications*, *30*(6), 453–458.

Grombe, R. (2009). Sulfated cellulose thin films with antithrombin affinity. *eXPRESS Polymer Letters*, *3*(11), 733–742.

Gutierrez, J., Tercjak, A., Algar, I., Retegi, A., & Mondragon, I. (2012). Conductive properties of TiO_2/bacterial cellulose hybrid fibres. *Journal of Colloid and Interface Science*, *377*(1), 88–93.

Håkansson, E., Amiet, A., Nahavandi, S., & Kaynak, A. (2007). Electromagnetic interference shielding and radiation absorption in thin polypyrrole films. *European Polymer Journal*, *43*(1), 205–213.

Hardy, J. G., Lee, J. Y., & Schmidt, C. E. (2013). Biomimetic conducting polymer-based tissue scaffolds. *Current Opinion in Biotechnology*, *24*(5), 847–854.

Hu, W., Chen, S., Yang, J., Li, Z., & Wang, H. (2014). Functionalized bacterial cellulose derivatives and nanocomposites. *Carbohydrate Polymers*, *101*, 1043–1060.

Hu, W., Chen, S., Yang, Z., Liu, L., & Wang, H. (2011). Flexible electrically conductive nanocomposite membrane based on bacterial cellulose and polyaniline. *Journal of Physical Chemistry B*, *115*(26), 8453–8457.

Janik, R., Kucharski, S., Sobolewska, A., & Barille, R. (2010). Chemical modification of glass surface with a monolayer of nonchromophoric and chromophoric methacrylate terpolymer. *Applied Surface Science*, *257*(3), 861–866.

Jung, Y. C., & Bhushan, B. (2006). Contact angle, adhesion and friction properties of micro- and nanopatterned polymers for superhydrophobicity. *Nanotechnology*, *17*(19), 4970–4980.

Kaur, A., Ishpal, & Dhawan, S. K. (2012). Tuning of EMI shielding properties of polypyrrole nanoparticles with surfactant concentration. *Synthetic Metals*, *162*(15–16), 1471–1477.

Kawakita, J., Hashimoto, Y., & Chikyow, T. (2013). Strong adhesion of silver/polypyrrole composite onto plastic substrates toward flexible electronics. *Japanese Journal of Applied Physics*, *52*(6)

Klemm, D., Schumann, D., Udhardt, U., & Marsch, S. (2001). Bacterial synthesized cellulose—Artificial blood vessels for microsurgery. *Progress in Polymer Science*, *26*(9), 1561–1603.

Lafuma, A., & Quere, D. (2003). Superhydrophobic states. *Nature Materials*, *2*(7), 457–460.

Lange, U., Roznyatovskaya, N. V., & Mirsky, V. M. (2008). Conducting polymers in chemical sensors and arrays. *Analytica Chimica Acta*, *614*(1), 1–26.

Li, N., Huang, Y., Du, F., He, X. B., Lin, X., Gao, H. J., et al. (2006). Electromagnetic interference (EMI) shielding of single-walled carbon nanotube epoxy composites. *Nano Letters*, *6*(6), 1141–1145.

Lin, Z., Guan, Z., & Huang, Z. (2013). New bacterial cellulose/polyaniline nanocomposite film with one conductive side through constrained interfacial polymerization. *Industrial & Engineering Chemistry Research*, *52*(8), 2869–2874.

Müller, D., Rambo, C. R., Recouvreux, D. O. S., Porto, L. M., & Barra, G. M. O. (2011). Chemical in situ polymerization of polypyrrole on bacterial cellulose nanofibers. *Synthetic Metals*, *161*(1–2), 106–111.

Marins, J. A., Soares, B. G., Barud, H. S., & Ribeiro, S. J. (2013). Flexible magnetic membranes based on bacterial cellulose and its evaluation as electromagnetic interference shielding material. *Materials Science and Engineering C*, *33*(7), 3994–4001.

Martins, N. C. T., Freire, C. S. R., Neto, C. P., Silvestre, A. J. D., Causio, J., Baldi, G., et al. (2013). Antibacterial paper based on composite coatings of nanofibrillated cellulose and ZnO. *Colloids and Surfaces A: Physicochemical and Engineering Aspects*, *417*, 111–119.

Nystrom, G., Mihranyan, A., Razaq, A., Lindstrom, T., Nyholm, L., & Stromme, M. (2010). A nanocellulose polypyrrole composite based on microfibrillated cellulose from wood. *Journal of Physical Chemistry B*, *114*(12), 4178–4182.

O'Lenick, A. J. (2000). Silicones—Basic chemistry and selected applications. *Journal of Surfactants and Detergents*, *3*(2), 229–236.

Omastova, M., & Micusik, M. (2012). Polypyrrole coating of inorganic and organic materials by chemical oxidative polymerisation. *Chemical Papers*, *66*(5), 392–414.

Pan, Y., Li, Z., Liu, T., Zheng, Z., Ding, X., & Peng, Y. (2012). Shape memory hydrogen-bonded P(MMA-co-HEA)/PDMS-OH complexes. *Acta Polymerica Sinica*, *2*, 131–137.

Pankaj, K., Kumar, S. H., & Sukhjeet, K. (2012). Conducting polymer based potentiometric sensors. *Research Journal of Chemistry and Environment*, *16*(3), 125–133.

Pickup, N. L., Lam, M., Milojevic, D., Bi, R. Y., Shapiro, J. S., & Wong, D. K. Y. (1997). Investigations of the feasibility of constructing a polypyrrole-mercury mercury chloride reference electrode. *Polymer*, *38*(10), 2561–2565.

Salazar-Hernández, C., Alquiza, M. J. P., Salgado, P., & Cervantes, J. (2010). TEOS-colloidal silica-PDMS-OH hybrid formulation used for stone consolidation. *Applied Organometallic Chemistry*, *24*(6), 481–488.

Sen, B., Hamelin, J., Bru-Adan, V., Godon, J. J., & Chandra, T. S. (2008). Structural divergence of bacterial communities from functionally similar laboratory-scale vermicomposts assessed by PCR-CE-SSCP. *Journal of Applied Microbiology*, *105*(6), 2123–2132.

Shukla, S. K. (2013). Synthesis and characterization of polypyrrole grafted cellulose for humidity sensing. *International Journal of Biological Macromolecules*, *62*, 531–536.

Takagi, S., Makuta, S., Veamatahau, A., Otsuka, Y., & Tachibana, Y. (2012). Organic/inorganic hybrid electrochromic devices based on photoelectrochemically formed polypyrrole/TiO_2 nanohybrid films. *Journal of Materials Chemistry*, *22*(41), 22181–22189.

Tang, H., Wang, H., & He, J. (2009). Superhydrophobic titania membranes of different adhesive forces fabricated by electrospinning. *Journal of Physical Chemistry C*, *113*(32), 14220–14224.

Tjahyono, A. P., Aw, K. C., & Travas-Sejdic, J. (2012). A novel polypyrrole and natural rubber based flexible large strain sensor. *Sensors and Actuators B—Chemical*, *166*, 426–437.

Varesano, A., & Tonin, C. (2008). Improving electrical performances of wool textiles: Synthesis of conducting polypyrrole on the fiber surface. *Textile Research Journal*, *78*(12), 1110–1115.

Wang, C., & He, X. (2006). Preparation of hydrophobic coating on glass surface by dielectric barrier discharge using a 16 kHz power supply. *Applied Surface Science*, *252*(23), 8348–8351.

Wang, H., Leaukosol, N., He, Z., Fei, G., Si, C., & Ni, Y. (2013). Microstructure, distribution and properties of conductive polypyrrole/cellulose fiber composites. *Cellulose*, *20*(4), 1587–1601.

Wang, Q., Wang, J., Lv, G., Wang, F., Zhou, X., Hu, J., et al. (2014). Facile synthesis of hydrophilic polypyrrole nanoparticles for photothermal cancer therapy. *Journal of Materials Science*, *49*(9), 3484–3490.

Wang, Y., & Jing, X. (2005). Intrinsically conducting polymers for electromagnetic interference shielding. *Polymers for Advanced Technologies*, *16*(4), 344–351.

Wen, L., Ma, Y., Dai, B., Zhou, Y., Liu, J., & Pei, C. (2013). Preparation and dielectric properties of SiC nanowires self-sacrificially templated by carbonated bacterial cellulose. *Materials Research Bulletin*, *48*(2), 687–690.

Yan, Z., Chen, S., Wang, H., Wang, B., & Jiang, J. (2008). Biosynthesis of bacterial cellulose/multi-walled carbon nanotubes in agitated culture. *Carbohydrate Polymers*, *74*(3), 659–665.

Yildiz, Z., Usta, I., & Gungor, A. (2012). Electrical properties and electromagnetic shielding effectiveness of polyester yarns with polypyrrole deposition. *Textile Research Journal*, *82*(20), 2137–2148.

Yuan, X., Ding, X., Wang, C., & Ma, Z. (2013). Use of polypyrrole in catalysts for low temperature fuel cells. *Energy & Environmental Science*, *6*(4), 1105–1124.

Zhang, W., Chen, S., Hu, W., Zhou, B., Yang, Z., Yin, N., et al. (2011). Facile fabrication of flexible magnetic nanohybrid membrane with amphiphobic surface based on bacterial cellulose. *Carbohydrate Polymers*, *86*(4), 1760–1767.

Zheng, W., Hu, W., Chen, S., Zheng, Y., Zhou, B., & Wang, H. (2014). High photocatalytic properties of zinc oxide nanoparticles with amidoximated bacterial cellulose nanofibers as templates. *Chinese Journal of Polymer Science*, *32*(2), 169–176.

Zhu, L., & Jin, Y. (2005). Preparation and performance of hydrophobic inorganic/organic film. *Surface Technology*, *34*(3), 1–4, 32.